Observation of a Large Steric Effect on the XeBr* Formation in the Reaction of Oriented CF_3Br with $Xe(^3P)$

H. Ohoyama,* R. Midorikawa, and T. Kasai*

Department of Chemistry, Graduate School of Science, Osaka University, Toyonaka, Osaka 560, Japan

Received: December 23, 1996; In Final Form: May 16, 1997[⊗]

A large steric effect on XeBr* formation was observed in the reaction of oriented CF_3Br with $Xe(^3P)$. The reaction cross-section was found to be largest for the Br-end collisons and smallest for the CF_3-end collisions, even though the electron transfer takes place at relatively large internuclear distances in the entrance channel. The large orientational dependence may be attributed to the fraction of the collisions that have small impact parameters which can lead to the formation of XeBr*. The majority of the collisions, having larger impact parameters, are supposed to lead to electron back-transfer in the exit channel and are relatively insensitive to the reactant orientation.

1. Introduction

The electric hexapole technique is one of the useful methods for selecting molecular orientation of symmetric tops. With use of this method, steric effects on chemical reactions have been widely investigated.[1] Most studies concern reactions of alkali metals and the alkaline earth metal atoms. For the reactions of alkali metals that lead to the formation of metal halides, the "harpoon" mechanism has been advanced.[2] Janssen and co-workers have studied the reactions of $Ca(^1D_2)$ with oriented CH_3X (X = F, Cl, Br) and observed a considerable steric effect for the $CaF(A^2\Pi)$ formation. The enhanced CaCl(B) formation was observed for the methyl-end orientation and the enhanced CaBr(A) formation for the Br-end orientation.[3] Orientation dependence has been studied for several chemiluminescent reactions. Jalink and co-workers investigated the Ba + N_2O reaction,[4] and van den Ende and Stolte measured the steric effect on the NO* formation in the reaction of oriented NO with O_3.[5]

The reactions of the metastable rare-gas atoms with small molecules have provided a long-standing interest because of their large quenching cross-sections and diversity of competitive reaction channels, i.e. electronic energy transfer, molecular dissociation, Penning ionization, and excimer formation. The steric effects on the several dissociative energy transfer reactions with metastable rare-gas atoms have been observed in our laboratory. The observed orientation dependences suggest that the electron exchange mechanism plays a role, and this is relevant to the spatial distributions of the reactant molecular orbitals.[6] Though rare-gas halide excimer formations with halogen-containing molecules are of great interest because of the analogy to the harpoon mechanism, the steric effect has been investigated only for a few systems, such as the Xe* + IBr reaction using laser-aligned molecules in photodissociation.[7] The reaction cross-section was found to be largest when Xe* approaches parallel to the plane of rotation of the IBr. The result was interpreted in terms of the anisotropy of the ionic $Xe^+ + IBr^-$ potential energy surface. The similarity between metastable rare-gas atoms and alkali metal atoms has been pointed out on the basis of the electronic structure.[8] On the other hand, the difference between the np^5 ion-core configuration of the metastable rare-gas atom and the np^6 of the alkali metal atom, or $np^6(n + 1)s$ of the alkaline earth metal atom, provides an interesting contrast because of repulsive nature of the exit potential for the ion pair. It is therefore important to study steric effects on the rare-gas halide excimer formation. We investigate steric efficts on the XeBr* formation in the reaction of oriented CF_3Br with $Xe(^3P)$.

2. Experimental Section

The apparatus and the experimental procedure have been described in detail elsewhere.[6] In brief, the 2-ms pulsed $Xe(^3P)$ beam was produced by an electric glow discharge with 30-V-dc potential and a stagnation pressure of 70 Torr at a pulsed valve. The 10-ms pulsed CF_3Br beam was produced by a supersonic expansion using a pulsed valve and a pressure of 500 Torr. The velocity distributions of CF_3Br and $Xe(^3P)$ were determined by a conventional time of flight (TOF) method. The TOF profiles were simulated with the shifted-Maxwellian distribution.[9] The parameters for the stream velocity and the spread of the velocity distribution were determined and found to be $v_s = 365$ ms^{-1}, $\alpha_s = 70$ ms^{-1} for the CF_3Br beam and $\gamma_s = 355$ ms^{-1}, $\alpha_s = 60$ ms^{-1} for the $Xe(^3P)$ beam, respectively. The CF_3Br beam was rotationally selected and focused by a 60-cm electric hexapole field followed by a guiding field and oriented at the beam intersection in an orienting field (100 V cm^{-1}). Though the strength of the orienting field could be relatively weak if we consider the quadrupole coupling constant for Br, which is ca. 600 MHz, it was found to be sufficient for the practical measurement.[10] The emission of XeBr(B,C) from the beam crossing zone was collected by a concave mirror through a long-pass filter (V-33, HOYA) and focused on a photomultiplier (R943-02, Hamamatsu Photonics). The signal is fed to a gated photon-counting system. The background counts were subtracted every time from the crossed beam signal. The difference counts were accumulated over 40 000 pulses by a microcomputer, until an acceptable signal-to-noise ratio was obtained. The molecular orientation was changed by switching the direction of the orienting field to positive, negative, and zero for every 300 beam pulses. The focusing curve was measured by a quadrupole mass spectrometer tuned to the CF^+ fragment peak ($m/e = 31$) in order to determine the orientational distribution of the CF_3Br, $W(\cos \gamma_0)$, where γ_0 is the orientational angle with respect to the relative velocity vector of collision. The chemiluminescence measurement was carried out

[⊗] Abstract published in *Advance ACS Abstracts,* September 15, 1997.

S1089-5639(97)00055-8 CCC: $14.00

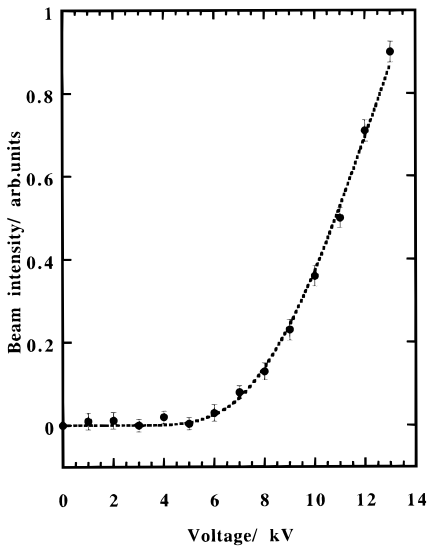

Figure 1. Focusing curve of the CF_3Br beam. The solid circles with an error bar are the expermental points. The dotted curve is calculated by a numerical trajectory simulation, including the second order Stark effect. The rotational distribution was assumed to be a Boltzmann distribution with a temperature of 45 K.

at a fixed hexapole rod voltage of 13 kV. Though the intensity of the focused beams was not much enhanced at 13 kV due to the small dipole moments of CF_3Br (0.64 D), a good degree of orientation could be achieved in return as we show in the following section.

3. Results

3.1. Orientational Distribution of the CF_3Br Beam. Figure 1 shows the focusing curve of the CF_3Br beam. The orientational distribution, $W(\cos\gamma_0)$, of CF_3Br was estimated by means of a numerical trajectory simulation of the focusing curve assuming a thermal distribution of rotational states. For a symmetric top molecule in a $|J,K,M\rangle$ state, the Stark effect up to second order is given by[11]

$$W_{\text{Stark}} = -\rho\mu E + \frac{\mu^2E^2}{2Bhc} f(J,K,M) \qquad (1)$$

where

$$\rho = \frac{KM}{J(J+1)}$$

$$f(J,K,M) = \frac{(J^2-K^2)(J^2-M^2)}{J^3(2J-1)(2J+1)} - \frac{[(J+1)^2-K^2][(J+1)^2-M^2]}{(J+1)^3(2J+1)(2J+3)}$$

Here, K and M give the projections of the rotational angular moment, J, on the molecular axis and the electric field axis, respectively, E is the magnitude of the electric field, μ is the permanent dipole moment of the molecule, and B is the rotational constant for rotations about an axis perpendicular to the molecular axis. Since the rotational constant of CF_3Br is small, the contribution of the second-order Stark to the beam focusing is considerably large, so that the simulation including the second-order Stark effect is required in the present simulation.[12] The numerical calculations of the molecular motion in the hexapole field were carried out for all $|J,K,M\rangle$ states up to 30 for J and K. The dashed line in Figure 1 is the calculated focusing curve with the rotational temperature of 45 K which is set equal to the measured translational temperature of the CF_3Br beam. The simulation was found to be in good agreement with the experimental data.

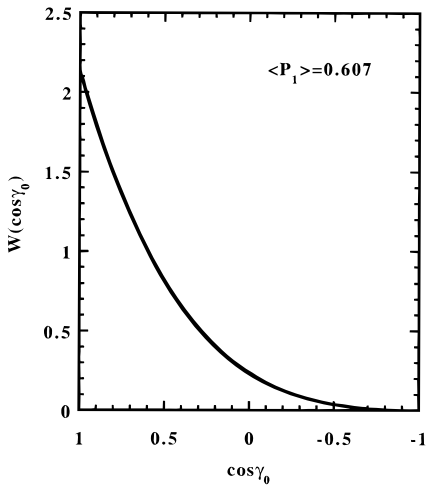

Figure 2. Estimated orientational distribution of the CF_3Br beam, after the state selection by a 60-cm hexapole field. Effects of depolarization due to the Br−quadrupolar coupling have been neglected in the orientating field of 100 V/cm.

TABLE 1: Orientation Dependence of XeBr* Emission Intensity

orientation	emission intens/(10^{-2} counts pulse^{-1})
Br end	3.95 ± 0.19
random	2.64 ± 0.20
CF_3 end	1.31 ± 0.19

Figure 2 shows the estimated $W(\cos\gamma_0)$ of the focused CF_3Br beam, taking the hexapole rod voltage of 13 kV and assuming a rotational temperature of 45 K. The calculated Legendre moments $\langle P_n\rangle$ of this orientational distribution are, $\langle P_0\rangle = 1.000$, $\langle P_1\rangle = 0.607$, $\langle P_2\rangle = 0.218$, $\langle P_3\rangle = 0.044$, $\langle P_4\rangle = 0.004$, and $\langle P_5\rangle = 0.000$. Since the Legendre expansion of $W(\cos\gamma_0)$ was found to converge rapidly, the expansion up to $n = 4$ turned out to be adequate for obtaining the proper orientational distribution. The typical uncertainty of the calculated Legendre moments is estimated to be less than 5% due to the uncertainty of the fit parameters. The degree of orientation of $\langle P_1\rangle = 0.607$ was practically sufficient to carry out the present experiment. Care must be taken however that the degree of orientation of the reagent is a function of the strength of the orienting field where the reaction occurs. Bulthuis et al. calculated such electric field dependence of various methyl halides and suggested that the degree of orientation for CF_3Br may decrease due to quadrupole interaction.[10] It is therefore likely that the practical degree of orientaition in the orienting field may be somewhat lower. This suggests that we would expect a larger steric effect than the one we obtain in the following.

3.2. Steric Effect of the XeBr* Emission. The dependence of the XeBr* emission intensity on the molecular orientation is summarized in Table 1. The reactivity at the Br end was found to be the largest. Collisions at the CF_3 end give an emission intensity which is smaller by a factor of 3. This dependence appears to be similar to the orientation dependence of the metal halide formation in the reactions of Rb + CH_3I and K + CF_3-Br, and these reaction cross-sections are regarded as being relatively small.[13,14]

In order to evaluate the observed steric effect on the the XeBr* formation, it is suitable to represent it in the form of a steric opacity function. The steric opacity function, $I(\cos\gamma_0)$,

TABLE 2: Steric Effect in the Three Reactive Zones

reactive zone	steric effect[a]
σ_h (Br end)	1.45 ± 0.15
σ_s (sideways)	1.18 ± 0.10
σ_t (CF_3 end)	0.19 ± 0.05

[a] The steric effect averaged over the orientation angle is defined as unity.

is defined as the reactivity of a molecule that has an orientational angle γ_0 with respect to the relative velocity vector of collison. In general, it is necessary to distinguish between $I(\cos \gamma_0)$ and $I(\cos \gamma_r)$. If the reaction occurs at a large distance, which is the case of the XeBr* formation, it is not straightforward to transform $I(\cos \gamma_0)$ to the intrinsic steric opacity function, $I(\cos \gamma_r)$, where the orientational angle γ_r is defined on the molecular frame. Only if the impact parameter is zero is γ_r equal to γ_0.

$$I = \int_{-1}^{+1} I(\cos \gamma_0)\, W(\cos \gamma_0)\, \mathrm{d} \cos \gamma_0$$

The observed normalized emission intensity, I, which is defined as the emission intensity divided by that for random orientation at a given hexapole rod voltage, is related to the steric opacity function.[15] Normally, a steric opacity function is determined by adjusting model parameters so as to reproduce the experimental results, as we will carry out in the following section.

3.3. Steric Opacity Function. The orientation dependence of the XeBr* emission was analyzed using two models in order to get the steric opacity function. One is the three-step function model, and another is the model using Legendre polynomials.

3.3.1. Three-Step Function Model. In the three-step function model, the CF_3Br molecule is supposed to have three distinct reactive zones, each extending over a γ_0 of 60°. The reaction probabilities in the three reactive zones are designated by σ_h, σ_s, and σ_t, for the Br end, the sideways, and the CF_3 end, respectively. In this model, the observed normalized emission intensity, I, is represented by the sum of the three reactive zones as given by the following equation.[16,17]

$$I = \int_{+0.5}^{+1} \sigma_h W(\cos \gamma_0)\, \mathrm{d} \cos \gamma_0 + \int_{-0.5}^{+0.5} \sigma_s W(\cos \gamma_0)\, \mathrm{d} \cos \gamma_0 + \int_{-1}^{-0.5} \sigma_t W(\cos \gamma_0)\, \mathrm{d} \cos \gamma_0$$

where $W(\cos \gamma_0)$ is the orientational distribution of the CF_3Br molecules in the orienting field. For random orientation, the emission intensity I should be equal to $(\sigma_h + 2\sigma_s + \sigma_t)/4$ which is set to unity. The reaction probabilities, σ_h, σ_s, and σ_t, can be determined by reproducing the normalized emission intensities of eq 2. The result is summarized in Table 2, and the obtained steric opacity function is represented by the solid line in Figure 3. A large steric effect is explicitly seen in the steric opacity function, $I(\cos \gamma_0)$, and the reactivity at the CF_3 end is found to be very small.

3.3.2. Legendre Fit. In this model,[6,15] only the firs term P_1 is found to be sufficient for reproducing the experimental result within the experimental error. It corresponds to the linear function model, which is expressed as follows.

$$I(\cos \gamma_0) = 1 + (0.76 \pm 0.06) P_1(\cos \gamma_0)$$

The obtained steric opacity function is also represented in Figure 3 by the dashed line. Just like in the three-step function model, a large orientation dependence with a large reactivity at the Br end and a very small reactivity at the CF_3 end is clearly seen.

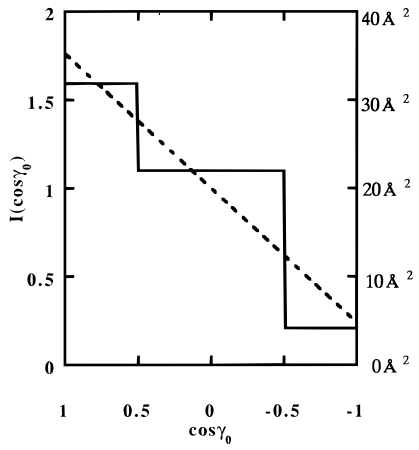

Figure 3. Steric opacity function for the XeBr* formation in the Xe(^{3}P) + CF_3Br reaction. Solid line: three-step function model. Dashed line: Legendre fit (the linear function model). The reaction cross-section averaged with respect to cos γ_0 is estimated to be 20 Å^2 for random orientation.[13]

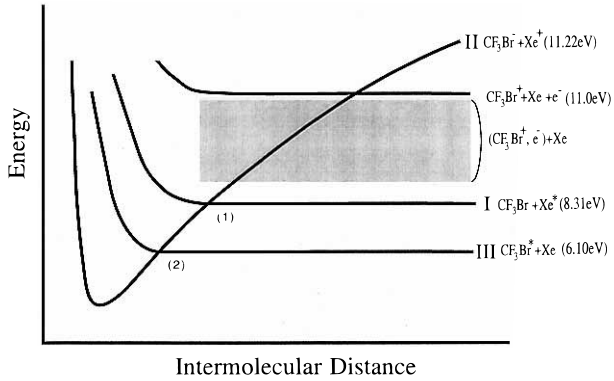

Figure 4. Potential energy curves of the Xe(^{3}P) + CF_3 Br reaction.

4. Discussion

Figure 4 shows a schematic two-body potential energy curve for the CF_3Br with Xe(^{3}P) reaction. The direct coupling of surface I of CF_3Br + Xe* with surfaces of the high Rydberg excited states, the shadow area of (CF_3Br^+, e^-) + Xe in Figure 4, is expected to be small because of large internuclear distances. It is thus plausible that surface I crosses the ionic surface II of CF_3Br^- + Xe^+ at crossing point 1. Under the circumstances, the XeBr* formation could be initiated by the "harpoon" mechanism as in the alkali metal reactions, where the cross-section is approximated as πr_c^2 by using r_c of eq 2,

$$e^2/r_c \cong \mathrm{IP(Xe(^3P))} - \mathrm{EA(CF_3Br)} \qquad (2)$$

where IP(Xe(^{3}P)) is the ionization potential of Xe(^{3}P), EA(CF_3-Br) is the electron affinity of CF_3Br, and r_c is the crossing distance between the covalent potential surface I and the ionic surface II.[2] The electron affinity of CF_3Br is 0.91 eV,[18] and the ionization potential of Xe(^{3}p) is 3.82 eV.[19] Equation 2 shows that the electron transfer must occur at a distance as large as $r_c \sim 5$ Å. The calculated values of r_c are listed in Table 3 for the XeBr* reaction and some related reactions. It is found that the CF_3Br + Xe(^{3}P) reaction has a larger r_c as compared with the metal halide reactions of K + CH_3I, Rb + CH_3I, and K + CF_3Br, and it is rather comparable to that of the K + CF_3I reaction. The latter has a large distance of the crossing point.

TABLE 3: List of Calculated r_c for Several Reaction Systems

reactions	ΔE(IP − EA)[a]	r_c/Å	πr_c^2/Å^2
Xe(^{3}P) + CF_3Br	2.91	5.0	79
K + CH_3I	4.32	3.5	38
Rb + CH_3I	3.98	3.6	41
K + CF_3Br	3.43	4.2	55
K + CF_3I	2.77	5.2	85

[a] Reference 18.

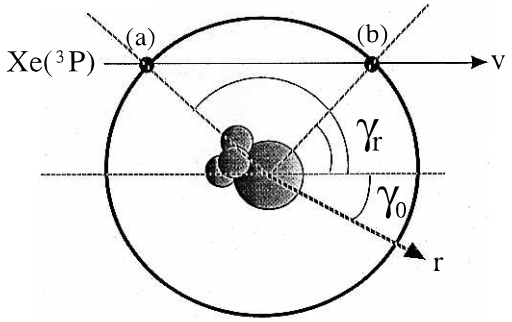

Figure 5. Schematic picture of the electron transfer in a collision with a large impact parmeter. The arrow **V** indicates a linear trajectory, and it encounters the ionic surface twice: point *a* near the CF_3 end and point *b* near the Br end. γ_0 is the orientational angle with respect to the relative velocity vector **V**. γ_r is the actual angle of attack of Xe(^{3}P) in the molecular frame. The impact parameter causes the actual angle of attcak γ_r to deviate from γ_0.

In the reactions with a relatively small crossing distance (r_c = 3.6 Å), Parker et al. observed a large steric effect for the backward scattering of RbI in the Rb + CH_3I reaction[13] and Carman et al. observed a large effect of molecular orientation on the KBr formation in the K + CF_3Br reaction (r_c = 4.2 Å).[14] However, only a small steric effect was observed for the K + CF_3I reaction with a relatively large crossing distance (r_c = 5.2 Å).[17] Even a larger value of 140 Å^2 rather than 79 Å^2 calculated from πr_c^2 has been reported for the total quenching cross-section of Xe(^{3}P) by CF_3Br. This suggests that the quenching occurs at an even larger distance and the attractive potential near crossing point 1 induces orbiting by virtue of a large coupling matrix element.[20] In this context, the large steric effect observed in the XeBr* formation is very surprising. We discuss more details about the cause of the large steric effect in terms of the category on the entrance channel and the exit channel.

4.1. Steric Effect in the Electron Transfer Process (The Entrance Channel). Following the harpoon mechanism, the reaction is induced by an electron jump from Xe(^{3}P) to CF_3Br. The electronic state of CF_3Br^- has been studied by electron spin resonance, and the unpaired electron is reported to stay in the antibonding σ^* orbital.[16,21] According to this assignment, the electron of the 6s orbital of Xe(^{3}P) would jump to the σ^* orbital of CF_3Br at crossing point 1. The energy of the σ^* orbital of CF_3Br is 4.9 eV, estimated from the excitation energy of 6.1 eV and the ionization energy of 11.0 eV for CF_3Br.[22−24] Similarly, the energy of the 6s orbital of Xe(^{3}P) is estimated to be 3.8 eV based on the excitation energy of 8.3 eV and the ionization energy of 12.1 eV for Xe.[19] Since both orbitals have nearly the same energy, a large coupling is expected at crossing point 1.

In a reaction with a large r_c, a large steric effect may not be expected because the electron gets the second chance to jump over again, as shown in Figure 5, where a simple case of the collision at the CF_3 end with a large impact parameter is shown. If the trajectory is assumed to be a linear trajectory, as indicated by the arrow, it encounters the ionic surface twice: point a near the CF_3 end and point b near the Br end. One might expect that the transfer efficiency for a collision with a large impact parmeter at the CF_3 end will be comparable with that of a collision at the Br end. Because the chance of the electron transfer may be even small at the first crossing point a, it could be large at the second crossing point b. Thus, the overall efficiency of the electron transfer at the CF_3 end turns out to be large in collisions with large impact parameters, and it could become comparable to that at the Br end.

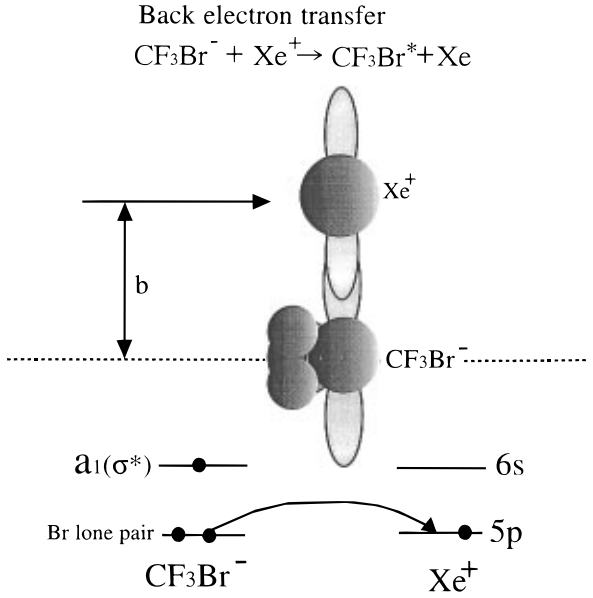

Figure 6. Schematic description of the back-electron transfer which occurs at crossing point 2 of Figure 4. The electron in the lone-pair orbital of CF_3Br^- transfers to the 5p orbital of Xe^+.

Analogously, only a small orientation dependence is seen for the forward scattering of RbI in the reaction of Rb with oriented CH_3I because of the large impact parameters.[13] The reactivities for the heads orientation and for the tails orientation are equal on the K + $CF_3I \rightarrow$ KI + CF_3 reaction, even though the angular distributions of KI for both orientations differ from each other.[17] Since the crossing distance for the Xe* + CF_3Br reaction is as large as that for the K + CF_3I reaction, it may be said that a large steric effect is not expected in the entrance channel. We therefore consider the steric effect in the exit channel, where more than two reaction channels compete.

4.2. Steric Effect on the Back-Electron Transfer Process (The Exit Channel). The branching fraction to the XeBr* excimer formation has been reported to be 0.14.[13] Thermodynamic considerations tell that there is no formation of CF_3* and Br* from the CF_3Br + Xe(^{3}P) reaction. Thus, the main process should be the formation of the excited state of CF_3Br*, and this is followed by the CF_3 + Br + Xe dissociation (dark channel). The absorption spectrum of CF_3Br indicates that only one electronic excited state of CF_3Br* (6.1 eV) can be accessible by the extra energy of Xe(^{3}P), and the transition is assigned to a transition from the lone-pair electron of the Br atom to the antibonding σ^* orbital of CF_3Br*.[22−24] Surface III could correlate with the dark channel because of the orbital character. Therefore, surface II crosses surface III at crossing point 2 shown in Figure 4, and this may lead the dissociative dark channel. This suggests that the excited state of CF_3Br* is produced via a back-electron transfer at crossing point 2.

The process of back-electron stransfer is illustrated in Figure 6. As previously mentioned, this process is the electron transfer from the lone-pair orbital of CF_3Br^- to the 5p orbital of Xe^+ at crossing point 2. The energy of the lone-pair orbital of CF_3Br^-

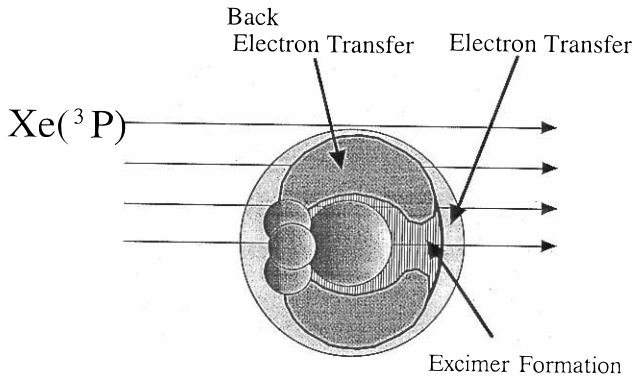

Figure 7. Summary of the proposed reaction mechanism. At crossing point 2, the large-impact-parameter collisions lead to the dissociative process of $CF_3 + Br + Xe$ via the back-electron transfer at the sideways region (dark areas), and the residual collisions with the small impact parameter are able to produce the XeBr* excimer (stripe area). The electron transfer at crossing point 1 is regarded as being isotropic, as indicated by the outer circle.

is estimated to be 11.0 eV from the ionization energy of CF_3Br,[22−24] and the estimated energy of the 5p orbital of Xe^+ is 12.1 eV.[19] Since both orbital energies are nearly equal, a large coupling matrix element between these surfaces is expected at crossing point 2. As a result, an effective back-electron transfer occurs and it gives a large fraction favor for the CF_3-Br* formation. In return, only a small fraction of 0.14 remains for the XeBr* excimer formation. This stresses the importance of the back-electron transfer in the exit channel. Since the lone-pair orbital is a p-orbital perpendicular to the molecular axis, the 5p orbital of Xe^+ can efficiently overlap with the lone-pair orbital for collisions at large impact parameters. For this reason, the coupling matrix element for the back-electron transfer is expected to be large in large-impact-parameter collisions. In contrast, the matrix element would become small for small-impact-parameter collisions. As a consequence, a large effect of molecular orientation is observed.

5. Conclusion

The proposed mechanism is sumarized in Figure 7. At crossing point 2, the collisons with large impact parameters efficiently go into the dissociative process of the $CF_3 + Br + Xe$ dark channel, and only the remaining part of the collisions with small impact parameters produce the XeBr* excimer on the diabatic pathway without the back-electron transfer. Therefore, the steric opacity function, $I(\cos \gamma_0)$, for the XeBr* formation reflects mostly the steric effect in the exit channel. The analogy on the electron transfer and/or the back-transfer processes could be applied to other relevant chemical reactions, such as the $O(^1D) + CF_3Br$ reaction.[25] Microscopic clarification on the correlation between stereodynamics and the nature of coupling at the crossing point of ionic and covalent potential energy surfaces may shed light for unveiling and controlling chemical reactions.[26]

Acknowledgment. The authors thank Dr. J. Bulthuis of Free University for his citical reading and time-consuming language correction of the manuscript. They also thank Professors F. Vecchiocattivi, V. Aquilanti, and A. Lagana of Perugia University for enlightening discussions about new aspects of the metastable atom reactions in experiment and theory. T.K. especially thanks Prof. Loesch of Bielefeld University for providing him stimulating scientific interactions at ZiF.

References and Notes

(1) Brooks, P. R. *Science* **1976**, 11. Stolte, S. *Ber. Bunsen-Ges. Physik. Chem.* **1982**, *86*, 413. Parker, D. H.; Bernstein, R. B. *Annu. Rev. Phys. Chem.* **1989**, *40*, 561. Levine, R. D.; Zweail, A.; El-Sayed, M. A. *J. Phys. Chem.* **1991**, *95*, 7961. Soep, B.; Vetter, R. *J. Phys. Chem.* **1995**, *99*, 13569. Kuwata, K.; Kasai, T. *The Chemical Dynamics and Kinetics of Small Radicals*, Part II; World Scientific: London, 1995; Chapter 12. Orr-Ewing, A. J. *J. Chem. Soc., Faraday Trans.* **1996**, *92*, 881. Loesch, H. J. *Annu. Rev. Phys. Chem.* **1995**, *46*, 555. Brooks, P. R. *Int. Rev. Phys. Chem.* **1995**, *14*, 327. Brooks, P. R.; Harland, P. W. In *Advances in Gas Phase Ion Chemistry*; Eds. Adams, N. G., Babcock, L. M. Eds.; JAI Press: Greenwich, CT, 1996; Vol. 2, p 1.

(2) Xing, G.; Kasai, T.; Brooks, P. R. *J. Am. Chem. Soc.* **1994**, *116*, 7421. Xing, G.; Kasai, T.; Brooks, P. R. *J. Am. Chem. Soc.* **1995**, *117*, 2581. Levine, R. D.; Bernstein, R. B. *Molecular Reaction Dynamics and Chemical Reactivity*; Oxford University Press: New York, 1987. Harland, P. W.; Carman, H. S., Jr.; Phillips, L. F.; Brooks, P. R. *J. Chem. Phys.* **1989**, *90*, 5201. Harland, P. W.; Carman, H. S., Jr.; Phillips, L. F.; Brooks, P. R. *J. Chem. Phys.* **1990**, *93*, 1089. Harland, P. W.; Carman, H. S., Jr.; Phillips, L. F.; Brooks, P. R. *J. Phys. Chem.* **1991**, *95*, 8137.

(3) Janssen, M. H. M.; Parker, D. H.; Stolte, S. *J. Phys. Chem.* **1991**, *95*, 8142. Janssen, M. H. M.; Parker, D. H.; Stolte, S. *J. Phys. Chem.* **1996**, *100*, 16066.

(4) Jalink, H.; Parker, D. H.; Meiwes-Broer, K. H.; Stolte, S. *J. Phys. Chem.* **1986**, *90*, 552. Jalink, H.; Nicolasen, G.; Stolte, S.; Parker, D. H. *J. Chem. Soc., Faraday Trans. 2* **1989**, *85*, 1115.

(5) van den Ende, D.; Stolte, S. *Chem. Phys.* **1984**, *89*, 121.

(6) Ohoyama, H.; Kasai, T.; Ohashi, K.; Kuwata, K. *Chem. Phys.* **1992**, *165*, 155. Ohoyama, H.; Iguro, T.; Kasai, T.; Kuwata, K. *Chem. Phys. Lett.* **1993**, *209*, 361. Ohoyama, H.; Makita, H.; Kasai, T.; Kuwata, K. *J. Phys. Chem.* **1995**, *99*, 5798. Takahashi, H.; Ohoyama, H.; Kasai, T.; Nakano, M.; Yamaguchi, K. *J. Phys. Chem.* **1995**, *99*, 1985.

(7) de Vries, M. S.; Srdanov, V. I.; Hanrahan, C. P.; Martin, R. M. *J. Chem. Phys.* **1983**, *78*, 5582.

(8) Setser, D. W.; Dreiling, T. D.; Brashears, H. C., Jr.; Kolts, J. H. *Faraday Discuss. Chem. Soc.* **1979**, *67*, 255.

(9) Hagena, O. F.; Varma, A. K. *Rev. Sci. Instrum.* **1968**, *39*, 47. Anderson, J. B.; Andres, R. P.; Fenn, J. B. *Adv. Chem. Phys.* **1966**, *10*, 275.

(10) Bulthuis, J.; Milan, J. B.; Janssen, M. H. M.; Stolte, S. *J. Chem. Phys.* **1991**, *94*, 7181.

(11) Townes, C. H.; Shawlow, A. L. *Microwave Specrtoscopy*; Dover: New York, 1955; Chapter 10.

(12) Ohoyama, H.; Ogawa, T.; Kasai, T. *J. Phys. Chem.* **1995**, *99*, 13606.

(13) Parker, D. H.; Chakravory, K. K.; Bernstein, R. B. *Chem. Phys. Lett.* **1982**, *86*, 113.

(14) Carman, H. S.; Harland, P. W.; Brooks, P. R. *J. Phys. Chem.* **1986**, *90*, 944.

(15) Stolte, S.; Chakravorty, K. K.; Bernstein, R. B.; Parker, D. H. *Chem. Phys.* **1982**, *71*, 353.

(16) Hasegawa, A.; Williams, F. *Chem. Phys. Lett.* **1977**, *46*, 66.

(17) Brooks, P. R.; Mckillop, J. S.; Pippin, H. G. *Chem. Phys. Lett.* **1979**, *66*, 144. Brooks, P. R. *J. Phys. Chem.* **1993**, *97*, 2153. Brooks, P. R. *Faraday Discuss. Chem. Soc.* **1973**, *55*, 299.

(18) Lide, D. R. *Handbook of Chemistry and Physics*; 71st ed.; Chemical Rubber Co.: Boca Raton, FL, 1990.

(19) Moore, C. E. *Atomic energy levels*; U. S. Department of Commerce Circular; Government Printing Office: Washington, D.C., 1952; p 467.

(20) Velazco, J. E.; Kolts, J. H.; Setser, D. W. *J. Chem. Phys.* **1978**, *69*, 4357. Tamagake, K.; Setser, D. W.; Kolts, J. H. *J. Chem. Phys.* **1981**, *74*, 4286.

(21) Hasegawa, A.; Shiotani, M.; Williams, F. *Faraday Discuss. Chem. Soc.* **1977**, *63*, 157.

(22) Doucet, J.; Gilbert, R.; Sauvageau, P.; Sandorfy, C. *J. Chem. Phys.* **1975**, *62*, 336.

(23) Doucet, J.; Sauvageau, P.; Sandorfy, C. *J. Chem. Phys.* **1973**, *58*, 3708.

(24) Suto, M.; Lee, L. C. *J. Chem. Phys.* **1983**, *79*, 1127.

(25) Alagia, M.; Balucani, N.; Casavecchia, P.; Lagana, A.; Ochoa de Aspuru, G.; Van Kleef, E. H.; Volpi, G. G.; Lendvay, G. *Chem. Phys. Lett.* **1996**, *258*, 323.

(26) Aquilanti, V.; Cappelletti, D.; Pirani, F. *J. Chem. Phys.* **1997**, *106*, 1.